AD-A139 941 STUDIES OF METASTABLE MICROCRYSTALLINE AND GLASSY ALLOYS(U) MASSACHUSETTS INST OF TECH CAMBRIDGE R C O'HANDLEY ET AL. MAR 84 ARO-17643.11-MS 1/1

UNCLASSIFIED DAAG29-80-K-0068 F/G 11/6 NL

END

DATE FILMED

6 84

DTIC

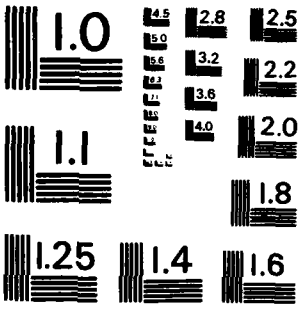

STUDIES OF METASTABLE MICROCRYSTALLINE AND GLASSY ALLOYS

FINAL REPORT

Professor Nicholas J. Grant, Principal Investigator

Dr. R. C. O'Handley, Principal Research Scientist

Professor K. H. Johnson, MIT

Professor R. M. Latanision, MIT

Professor B. C. Giessen, Northeastern University

March 20th, 1984

Submitted to U.S. Army Research Office
Research Traingle Park, NC 27709

Attn. Dr. P. Parrish

DAAG29-80-K-0088

Massachusetts Institute of Technology,
Cambridge, MA 02139

Unclassified

SECURITY CLASSIFICATION OF THIS PAGE (When Data Entered)

REPORT DOCUMENTATION PAGE	READ INSTRUCTIONS BEFORE COMPLETING FORM
1. REPORT NUMBER	2. GOVT ACCESSION NO. AD-A139 941 / 3. RECIPIENT'S CATALOG NUMBER
4. TITLE (and Subtitle) STUDIES OF METASTABLE MICROCRYSTALLINE AND GLASSY ALLOYS	5. TYPE OF REPORT & PERIOD COVERED FINAL REPORT
	6. PERFORMING ORG. REPORT NUMBER
7. AUTHOR(s) R. C. O'Handley & N. J. Grant	8. CONTRACT OR GRANT NUMBER(s) DAAG29-80-K-0088
9. PERFORMING ORGANIZATION NAME AND ADDRESS	10. PROGRAM ELEMENT, PROJECT, TASK AREA & WORK UNIT NUMBERS
11. CONTROLLING OFFICE NAME AND ADDRESS U. S. Army Research Office, Post Office Box 12211, Research Triangle Park, NC 27709	12. REPORT DATE March 1984 / 13. NUMBER OF PAGES
14. MONITORING AGENCY NAME & ADDRESS(if different from Controlling Office)	15. SECURITY CLASS. (of this report) Unclassified / 15a. DECLASSIFICATION/DOWNGRADING SCHEDULE

16. DISTRIBUTION STATEMENT (of this Report)

Approved for public release; distribution unlimited.

17. DISTRIBUTION STATEMENT (of the abstract entered in Block 20, if different from Report)

18. SUPPLEMENTARY NOTES

The view, opinions, and/or findings contained in this report are those of the author(s) and should not be construed as an official Department of the Army position, policy, or decision, unless so designated by other documentation

19. KEY WORDS (Continue on reverse side if necessary and identify by block number)

Rapidly solidified alloys
Microcrystalline alloys
Amorphous metals, glassy alloys
Magnetic metallic glasses
Microcrystalline aluminum alloys
Glass formation & stability

20. ABSTRACT (Continue on reverse side if necessary and identify by block number)

Results of broad inter- and intra-disciplinary research on metastable microcrystalline and glassy alloys are reported. Progress is noted in processing of R.S. aluminum alloys and in understanding and improving their corrosion resistance and mechanical properties. New metallic glasses with improved magnetic properties are described. Significant advances in understanding of bonding, glass formation stability and transformation in glassy materials through molecular-orbital cluster calculations are summarized.

DD FORM 1 JAN 73 1473 EDITION OF 1 NOV 65 IS OBSOLETE

UNCLASSIFIED

SECURITY CLASSIFICATION OF THIS PAGE (When Data Entered)

I PROJECT SUMMARIES

A. PROCESSING

1. ULTRASONIC GAS ATOMIZATION, P. K. Domalavage

A second generation USGA tank was designed, constructed and put into operation. It features simpler internal construction, greater crucible/pour tube flexibility and an improved cyclone collector. Later modifications have allowed us to extend the upper melt temperature limit to approximately 1750 degrees C.

In addition to extensive atomization of various aluminum alloys, we made the first reported dry atomization of a ferromagnetic metallic glass. The product showed a normal distribution of particle sizes with glassy alloy obtained for particles up to approximately 63 microns in diameter. This implies appreciable undercooling during the USGA process and points dramatically to the significant differences between USGA and melt spinning in terms of the relevant mechanisms for rapid solidification.

B. RAPIDLY SOLIDIFIED ALUMINUM ALLOYS

W. Wang, S. Kang, W. Webster, Y. Gefen and N. J. Grant

1. PHYSICAL PROPERTIES

A significant number of aluminum alloys were prepared primarily from RS powders, using hot extrusion for final consolidation. The alloys included new compositions as well as more heavily alloyed conventional grades such as 2024 and 7075. Important findings worthy of comment follow:

a) Alloy 2024 with additions up to 3% Li were prepared as RS-PM products and reproduced results obtained in earlier studies with twin roller splat foils. The powders were very much easier to handle and process than were the splat foils, however this might not be true with large scale production facilities (Wang and Grant: 2nd Int'l. Aluminum-Lithium Conf. Proc. 1983).

b) Al-6l7 Mg-1.6 Li was prepared from RS-PM powders by hot extrusion. Substituting Mg for about 4.5% Cu results in a much lower density alloy which enhances specific strength and specific modulus values. Unfortunately, in the Al-Mg-Li system alloy strengthening is based on precipitation of the δ Al_3Li phase which is subject to undesirable shear localization during deformation. Nevertheless attractive strength, modulus, and specific strength and modulus values were reported with only average fracture toughness properties. Furtherwork is warranted and recommended using modified compositions which will minimize the problems associated with shear localization of the Al_3Li phase (Wang and Grant: to be published)

c) RS-PM X2020 Alloys The Al-Cu-Li alloys with 1 to 3% Li do indeed develop excellent tensile and fatigue properties; however, fracture toughness properties are relatively poor. In spite of what appear to be useful high ductility values in smooth bar tensile tests, the fracture toughness behavior is disproportionately poor. Careful metallographic studies clearly show that the fault lies in the disproportionate amount of oxide formed in preparing these alloys. The presence of 3 to 11 atom pct of Li leads to formation of $LiAlO_2$ instead of Al_2O_3, resulting in a thicker, less protective oxide. The oxide is ultimately dispersed as stringers in the extruded alloy. With the limited amounts of hot reduction possible in small laboratory extrusions, the oxide stringers are inadequately dispersed and contribute severely to the poor toughness properties. Processing techniques to eliminate or minimize the oxide stringer effect will be pursued. (Kang and Grant, to be published).

d) RS-PM X7091 Aluminum Alloy. Because most of the original development was done with air atomized or combustion gas atomized RS powders, this X7091 alloy was produced from USGA inert gas atomized powders. Further, the USGA powders were slightly coarser, but were made as much smaller extrusions; this led to lower oxide content in the USGA alloy but also resulted in a much smaller extrusion ratio, which gave a poorer oxide dispersion. As a non-lithium containing alloy, ductilities and fracture toughness values were excellent and roughly equivalent to those reported for the air-atomized large extrusions. There is distinct need for studies of larger extrusions of RS-PM alloys than is common for laboratory experiments to thoroughly evaluate the role of the hot reduction on oxide dispersion and the resultant properties, particularly toughness properties. (Webster and Grant: to be published).

e) Structure-Property Relationships in RS-PM 7075 + 1%Ni + 1%Zr

One of the advantages of the RS-PM process is the ability to sharply increase the amount and type of alloying in already heavily alloyed commercial ingot grades of alloys, without loss of hot work ability and formability and without necessarily sacrificing ductility and toughness. The 7075 + Ni+Zr alloy is an excellent illustration of the potential. Yield strength values near 100,000 psi with ultimate tensile strengths near 108,000 psi, with excellent ductility, notch tensile to yield ratios well in excess of 1.0 and attractive fatigue crack growth rates, especially at low crack rates. From any point of view we believe that this alloy could, today, be considered for commercial study and application. Further studies are under way with this alloy (Domalavage, Gefen and Grant: *Met. Trans. A.* 14A, 1983).

B.2 LIQUID DYNAMIC COMPACTION

E. J. Lavernia and N. J. Grant

As a means of simplying the conversion of atomized liquid metals and alloys; as a means of decreasing costs of consolidation of atomized material to intermediate product; and as a means of avoiding oxidation of the atomized

particulates during quenching of the powders to room temperature, liquid dynamic compaction is being studied to produce either shaped preforms (for rolling and extrusion) or intermediate products (ingots, billets, sheet strip).

A modified 7075 aluminum alloy containing 1% Ni and 1% Zr, was successfully produced by Liquid Dynamic Compaction (LDC) processing. The principal parameters of LDC were investigated, namely gas atomization pressure and substrate-to-nozzle distance. Densities of the as-deposited materials were as high as 95%, and the material was readily fully densified by a 28/1 extrusion ratio (area) at 400°C. No variation in hardness throughout the cross section of the as-deposited preform (about 2.5 cm thick) was found. Most importantly, porosity was micron size, broadly dispersed and oxide free, not interconnected. The as-deposited product was fine grained, free of directional growth patterns and highly plastic.

A fine cell structure of 10-12 μm in the as-deposited material suggests a solidification rate of about 10^3 °C/sec. The cell structure was equiaxed in all spatial directions and no prior particle or droplet boundaries were observed, due in part to the splat deformation of the semi-liquid droplets and the absence of refractory oxide films on the liquid droplets.

Absence of delaminations in the fracture surface of fully compacted (densified) LDC deposits were noted and attributed to the absence of oxide stringers in the hot worked LDC product.

It is noteworthy that LDC of alloy 7075+Ni+Zr showed significantly improved room temperature properties (UTS 118 ksi, Y.S. 107 ksi, Elong. 8.6%) when compared with the properties of the ingot cast material (UTS 109, Y.S. 105, Elong. 1%).

In summary, it has been demonstrated that combining the steps of atomization and consolidation into a single process (LDC) is a useful way of controlling surface oxides while at the same time retaining the grain-refinement benefits of rapid solidification.

B.3 CORROSION RESISTANCE

A. Saito and R. M. Latanision

During the course of this research program, our interest has been directed toward the resistance of RSP aluminum alloys to uniform and localized corrosion and stress corrosion cracking. These studies are summarized below:

a) Resistance of RSP Aluminum Alloys to Uniform and Localized Corrosion

STATEMENT OF PROBLEM: The corrosion behavior of microcrystalline aluminum alloys has been studied in solutions of 0.1N H_2SO_4 + 0.5N Na_2SO_4 with and without chloride additions.

In a chloride-free solution, the naturally aged microcrystalline 2618 aluminum alloys had better corrosion resistance than the artificially aged microcrystalline alloys, but poorer corrosion resistance than the artificially aged conventional alloys. Pitting resistance of the microcrystalline alloys in the solution of 1000 ppm NcCl was better than that of the conventional alloys. It was found that pits initiated at the interfaces of the constituent particles FeNiAlg in the alloys that were aged at relatively low temperatures. Pits initiated at the grain boundaries in the alloys which were aged at higher temperatures. The pitting potentials of RSP and conventionally processed alloy 2618, given various thermal treatments, are shown as a function of solution chloride content in Figure 1.

Similar studies have been performed on aluminum alloy 2024 and Li-containing 2024, both processed by RSP as well as by conventional means. In chloride-free solutions, the microcrystalline and conventionally processed alloys with the same aging treatment had similar corrosion resistance in both cases. Pitting potentials in solutions with NaCl were not changed by aging and there was no difference in the pitting potentials of the microcrystalline and the conventional alloys in both instances. However, in the 2024 alloy, lithium additions were found to increase the corrosion rate and to decrease the pitting potentials. The pit initiation sites in the 2024 alloy were at particles of $CuMgAl_2$. In the Li-containg 2024 alloy, pit initiation in both the conventionally processed and RSP alloys occurs at a second phase which appears to include Cu, Mg, Al, and Li as components, perhaps explaining why the pitting potential was not affected by processing.

b) Stress Corrosion Cracking of RSP Aluminum Alloys

STATEMENT OF PROBLEM: The objective of this research is to determine the role of grain size (and, in particular, the fine grain size achieved through rapid solidification processing) in determining the mechanical behavior of materials in aqueous environments. Recent work has focused on an Al-Zr-Mg alloy.

The present state-of-the-art in stress corrosion cracking (SCC) of Al alloys has been extensively reviewed and meetings have been held with researchers active in this area. In the high strength 7000 series alloys there is increasing evidence that the SCC susceptibility of the material is closely related to the precipitate morphology at the grain boundaries and to the accumulation of grain boundary segregation. Rapid solidification may alter precipitate morphology and segregation at the boundary due to the increased grain boundary area in the fine grained material. Also, since the RSP material is generally more homogeneous than its conventionally processed counterpart, one would expect more uniform precipitation throughout the material reducing the amount of precipitate at the grain boundary. Finally, since SCC of 7000 series alloys occurs along the grain boundaries, the finer the grain size the more circuitous will be the crack path thus making crack propagation more difficult. The result may be a material with high strength and greater resistance to SCC.

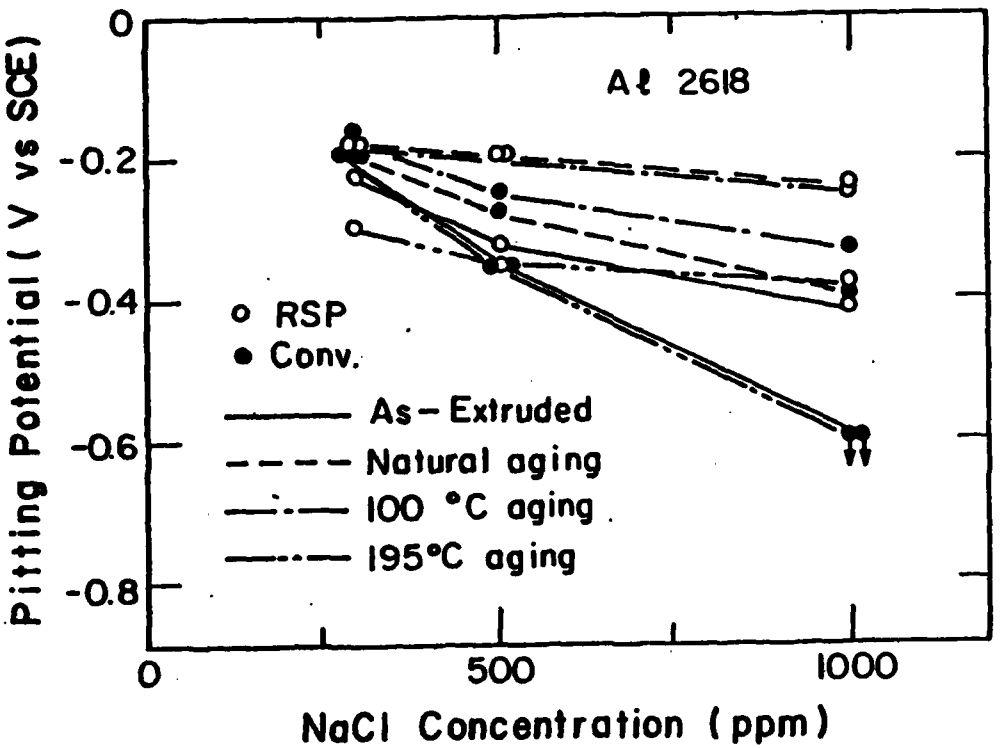
Al 2618
Pitting Potential (V vs SCE)
0
-0.2
-0.4
-0.6
-0.8
o RSP
• Conv.
As-Extruded
Natural aging
100 °C aging
195°C aging
0
500
1000
NaCl Concentration (ppm)

FIGURE 1

Based on these important findings, and their far-reaching implications, work is continuing in this crucial area.

To summarize, our results have led us to a better understanding of the micromechanisms leading to improved resistance to corrosion and to stress-corrosion cracking in certain RS alloys.

C. GLASSY ALLOYS

1. Ni_{40-60} Nb_{60-40} AMORPHOUS ALLOYS: THE ROLE OF ALLOYING ADDITIONS ON GLASS FORMING TENDENCIES AND THE CRYSTALLIZATION KINETICS

L. Collins and N. J. Grant

Ni-Nb glassy alloys were a focus of interest because of their high thermal stability among metallic glasses. While the kinetics of crystallization of these alloys followed the Johnson-Mehl-Avarami time dependence like most metallic glasses, the time exponent was only a third of that usually observed. We now see this as related to the complex crystal structure of the final product phases of the crystalline process. Furthermore the high activation energies for this class of metallic glasses (E = 660 kJ/mole) is seen to be a consequence of the stronger bonding between early and late transition metal species compared with that between transition metals and metalloids.

Ternary additions to this alloy system generally confirmed this new picture of glass stability. One result still difficult to reconcile with this view, however, is the observation that additions which served to increase the valence difference between the components reduced the crystallization temperature while easing glass formation.

C.2 NOVEL BORIDE DISPERSION HARDENED STAINLESS STEELS VIA CRYSTALLIZATION FROM THE AMORPHOUS STATE

C. Ashdown and N. J. Grant

The purpose of this study was to study the production of extremely fine grained, dispersion hardened stainless steels. Fe-25Cr-20Ni-12 a/o B was identified as a desirable composition both for glass formation and crystallization as well as for attainment of a ductile microcrystalline product. The RS ribbons were produced by melt spinning using a water cooled

Cu wheel. Quantities of 2 Kg or more with greater than 95% yield were attained for a number of compositions. As the extrusion temperatures of the alloy were reduced, finer grain sizes and finer boride dispersions were obtained. This effort culminated in material extruded at 800°C which had a 0.25 μm grain size, with 30 vol% borides (0.20 μm diameter) which provided both strengthening and grain boundary stability.

The 800°C extrusion displayed yield and tensile strengths of 210 and 225 Ksi, and an elongation and an R.A. of 3 and 5%, respectively. Warm swaging at 800°C reduced the yield and tensile strengths to 187 and 213 Ksi, but doubled the ductility values. This material is superplastic with elongations of up to 500% at 1100°C. More importantly, from a practical standpoint, superplastic tendencies persisted to temperatures as low as 800°C, still at strain rates as high as 10^{-2} sec^{-1}. The fine grain size is not stable at temperatures in excess of 800°C for the usual very slow strain rates for superplastic behavior, namely 10^{-3} to 10^{-5} per sec.

The oxidation behavior of these alloys was better than that of type 304, stainless steel. Modified with Si additions, the alloy was as good as stainless alloy 310 at 1000°C. The general corrosion resistance in sulphuric acid was comparable to that of 304, but the pitting resistance in chloride solutions was markedly inferior due to preferential dissolution of the matrix.

To summarize, markedly stronger stainless steels have been produced, with acceptable ductility. Superplastic forming is not only possible, but takes place at very low temperatures and very high strain rates. Oxidation and general corrosion resistance are good, but the pitting resistance is inferior. Further alloying with molybdenum and other elements should improve the pitting resistance.

C.3 THEORETICAL INVESTIGATIONS

M. E. Eberhart and K. H. Johnson

a) A Molecular-Orbital Model for Glass Formation and Melting of Amorphous Alloys

Recent self-consistent-field X-alpha scattered-wave (SCF-Xα-SW-molecular-orbital calculations on clusters representative of the structure of good metallic glass formers, notably Pd-Si, Cu-Zr, and Ni_2B, have revealed striking similarities among these alloys in terms of the molecular-orbital topology near the Fermi energy. In all the clusters, the molecular orbital immediately above the Fermi energy is bonding between the metalloid atoms in Pd-Si and Ni-B and between the Zr atoms in Cu-Zr. In all cases, these bonding interactions are representative of second-neighbor bonds. The next highest lying unoccupied molecular orbital, in all cases, is the antibonding counterpart of the bonding orbital. Whenever a bonding orbital and its antibonding counterpart occur consecutively within a molecular-orbital manifold, then that portion of the manifold has converged, and the nature of the molecular orbitals for a crystal of any size is fully determined within that portion of the manifold. In the case of Ni_2B, for example

the region immediately above the Fermi energy is bonding between each B atom. The molecular orbitals of higher energy have an increased number of boron-boron antibonding interactions, with the orbital that is antibonding between each pair of boron atoms marking the endpoint of this region of the molecular-orbital manifold. The process of heating a crystal will have two effects: the first is to thermally excite electrons into orbitals above the Fermi energy, resulting in a narrowing of the bonding-antibonding splitting through relaxations; the second is to excite phonons. In terms of the electronic structure, phonons will perturb the molecular orbitals, and this will also result in a narrowing of the bonding-antibonding splitting. When the second-neighbor bonding and antibonding interactions become degenerate as a result of these two processes, then there are no net second neighbor interactions, i.e., they are nonbinding. This is the melting point, for in the absence of second-neighbor interactions, non-space filling local structures will be as energetically favorable as the crystal structure.

b) Molecular-Orbital Model for the Electrical Resistivity of Amorphous Co-Mn-B Alloys

SCF-Xα-SW cluster molecular-orbital calculations have been carried out for amorphous Co-Mn-B alloys in order to explain a "step-like" decrease in the electrical resistance at 5 at.% Mn, superimposed on an overall increase in resistance, as measured by O'Handley at MIT. The SCF-Xα-SW studies suggest that at 5 at.% Mn, the Mn atoms are sufficiently close to form Mn-Mn bonds. This interaction lowers previously unoccupied B-Mo bonding orbitals below the Fermi energy resulting in increased B-Mn bonding and a corresponding shortening of the B-Mn distance causing an increase in the density of this metallic glass. There are three possible explanations for the change in resistivity accompanying the change in density: first the lowering of levels due to the Mn-Mn interactions opens up new conduction channels; second, the occupying of additional Mn-B bonding orbitals would increase the Mn-bond force constant, thus decreasing the phonon scattering cross section; third, the occupying of additional Mn-B bonding orbitals might form a more ordered Mn-B sub-structure, thus decreasing the overall disorder of the glassy structure.

c) Molecular-Orbital Model for Structural Phase Transitions in Crystalline and Amorphous Cobalt Alloys.

SCF-Xα-SW molecular-orbital calculations have been carried out for clusters representative of cobalt-rich amorphous alloys. The results suggest that there are two nearly degenerate electronic configurations for 12-fold coordinated cobalt. The fact that neither of these configurations corresponds to a cluster that is necessarily space filling indicates that the transitions from one of these structures to another will not be observable in the crystalline phase. However, in the amorphous materials these transitions should be observable. Transitions between the two configurations provide a fully consistent model for first-order structural phase transition in cobalt-rich amorphous alloys. It has also been found that the structural phase transition from hcp to fcc crystalline cobalt can be interpreted as resulting from a John-Teller process.

In summary, our calculations on a variety of clusters representative of the glassy state have provided dramatic new insights into stability, into electrical and magnetic properties and into local structural transformations of the materials in a way not possible through other calculational techniques.

C.4 MAGNETIC PROPERTIES

B. W. Corb and R. C. O'Handley

The problems addressed in this phase of the program were 1) furthering our understanding of the electronic interactions important to magnetic properties and to glass formation/stability and 2) developing the potential of novel low metalloid metallic glasses for high frequency applications. This second goal necessarily focussed on the importance of zero magnetostriction for such applications.

We pioneered in developing new low-metalloid glasses such as $Co_{80}Nb_{14}B_6$. Our efforts, we learned later, were paralleled by concurrent work in Japan. We showed that these new low-magnetostriction soft magnetic alloys derived their superior stability from a bonding interaction between their early and late transition metal constituents. The low dc coercivities observed in these glasses in their as-cast state (typically 0.05 Oe) are not degraded with increasing frequency as quickly as is the case for typical metallic glasses commercially available.

Our close and fruitful interaction with Professor Johnson further seeded the formulation of a new phenomenological model interpreting magnetic properties and bonding within a common framework. This new model affords more than just hindsight in structure-property relations. It allowed us to predict magnetic moments, and, to a certain extent, alloy stability in compositions containing metalloids other than boron.

A novel low-temperature, reversible transformation within the glassy state was discovered in several members of the Co-Nb-B series. Observation and interpretation of this transformation has fostered new insights into the local atomic order of amorphous alloys. One manifestation of the transformation is an abrupt vanishing of magnetostriction upon transformation of Co-Nb-B to a different glassy structure at approximately 100 degrees C. The potentially useful and the possibly deleterious technological implications of such transformations are being actively investigated. Important connections with work elsewhere on other metallic glass sytems is beginning to add to the general context in which these transformations would be considered.

D. NORTHEASTERN SUBCONTRACT

HYDROGEN IN METALLIC GLASSES

B. C. Giessen, S. Whang, R. Finocciaro, Northeastern University

II PERSONNEL

Nicholas J. Grant
Peter K. Domalavage
B. C. Giessen (Northeastern University)
K. H. Johnson
R. M. Latanision
R. C. O'Handley

Charles Ashdown
B. W. Corb
M. E. Eberhart
R. Finocciaro (Northeastern University)
Y. Gefen
S. Kang
A. Saito
W. Wang
W. Webster

L. Collins

E. Lavernia

S. Whang (Northeastern University)

Degrees granted:

Ph.D.	M.S.
C. Ashdown '84	W. Webster '82
B. W. Corb '83	
L. Collins '81	
S. Kang '82	
W. Wang '81	
M. E. Eberhart '83	
R. Finocciaro '83 (NU)	

III BIBLIOGRAPHY

Papers published:

1. A Molecular Orbital Model of Melting and Glass Formation. M. E. Eberhart, K. H. Johnwon and R. C. O'Handley. In: *Rapidly Solidified Amorphous and Crystalline Alloys*, B. H. Kear and B. C. Giessen and M. Cohen (eds.) New York, Elsevier North-Holland, 1982, pp. 103-108.

2. New Magnetic Alloys with Reduced Metalloid Content. R. C. O'Handley and N. J. Grant. In: *Rapidly Solidified* op cit., pp. 217-223.

3. Fundamental Magnetic Properties. R. C. O'Handley. In: *Amorphous Metallic Alloys*, F. E. Luborsky (ed.), London, Butterworth, 1983, p. 257.

4. Structural Relaxation and Curie Temperature of Fe-B Metallic Glasses. F. F. So, R. Kaplow and R. C. O'Handley. *J. Non-cryst. Sol.* 58: 285, 1983.

5. Chemical Bonding, Magnetic Moments and Local Symmetry in Transition-Metal Metalloid Alloys. B. W. Corb, R. C. O'Handley and N. J. Grant. *Phys. Rev.* 27:636, 1983.

6. Chemical Bonding and Local Symmetry in Co- and Fe-metalloid Alloys. B. W. Corb, R. C. O'Handley and N. J. Grant. *J. Appl. Phys.* 53: 7728, 1982.

7. Magnetic Properties of Some New Co-Nb-B Glasses. R. C. O'Handley, B. W. Corb, Y. Hara, N. J. Grant, and W. A. Hines. *J. Appl. Phys.* 53:7753, 1982.

8. Resistivity of Amorphous Co-Mn-B Alloys: Beyond the s-d Model. R. C. O'Handley, M. E. Eberhart, K. H. Johnson, and N. J. Grant. *J. Appl. Phys.* 53:8231, 1982.

9. Amorphous and Microcrystalline $Cu_{06}Zr_{04}$ Powders Made by Ultrasonic Gas Atomization. P. Domalavage, C. Ashdown, R. C. O'Handley and N. J. Grant. *J. Mater. Sci. and Eng.* 57:L1, 1983.

10. Magnetic Moments and Bonding in Amorphous Co-Nb-B Alloys. B. W. Corb, R. C. O'Handley, N. J. Grant, and V. L. Moruzzi. *J. Mag. Magn. Mater.* 31-34:1537, 1983.

11. Ultrasonic Gas Atomized Powders of Magnetic Alloys. R. C. O'Handley, P. Domalavage, B. W. Corb, Y. Hara, and N. J. Grant. In: *Rapid Solidification Processing: Principles and Technologies, III.* Robert Mehrabian (ed.), Washington, D.C., National Bureau of Standards, 1983, pp. 678-685.

12. Magnetoelastic Evidence for a Local Structural Transformation in Co-Rich Glasses. R. C. O'Handley and N. J. Grant. *Physica,* 11B:173, 1983.

13. First-Order, Structural Transformations in Metallic Glasses. *Phys. Rev. Lett.* 51:1386-1389, 1983.

14. Reversible Transformations of Short-Range Order in Cobalt-Base Glasses. R. C. O'Handley, R. W. Corb, J. Megusar, and N. J. Grant: *J. Non-cryst. Solids,* 61 & 62:773-780, 1984.

15. Molecular Orbital Models of Structural Phase Transitions in Crystalline and Amorphous Cobalt Alloys. M. E. Eberhart, R. C. O'Handley and K. H. Johnson. *Phys. Rev.*

16. Crystallization of amorphous $Ni_{60}Nb_{40}$. L. E. Collins, N. J. Grant, J. B. Vander Sande. *J. Mater. Sci.* 18:804-814, 1983.

17. Annealing Effects and Homogeneous Flow in $Ni_{60}Nb_{40}$ Metallic Glass. *Mater. Sci. Eng.* 61:137-147, 1983.

18. Rapid Solidification of Metallic Particulates. N. J. Grant. *J. Metals*, 35:20-27, 1983; and in: *High-Strength Aluminum Powder Metallurgy*. Michael J. Koczak and Gregory J. Hildeman (eds.), Metals Park, Ohio, TMS-AIME, 1983, pp. 3-18.

19. Corrosion Resistance of Rapidly Quenched Alloys. R. M. Latanision, A. Saito, and R. Sandenbergh. In: *Chemistry and Physics of Rapidly Solidified Materials*. Metals Park, Ohio, TMS-AIME, 1983, p.153.

20. Thermodynamic Properties of Dilute Solutions of Hydrogen in Glassy $Pd_{80}Si_{20}$. R. S. Finocciaro, C. L. Tsai and B. C. Giessen. In: *Rapidly Solidified* op. cit. pp. 243-248.

21. Effects of Alloying Additives on the Hydrogen Absorption Isotherms of Pd-Si. R. S. Finocciaro, C. L. Tsai and B. C. Giessen. MRS, 1981.

22. Compositional Effects on Hydrogen Embrittlement of Fe-base Glassy Metals. S. H. Whang, R. S. Finocciaro and B. C. Giessen. *Scripta Met.*

23. Compositional Dependence of the Thermodynamic Properties of Glassy Pd-Si Hydrides. R. S. Finocciaro and B. C. Giessen. *J. Less Common Metals,*

24. Magnetostriction and the local order of Co-Nb-B glasses. B. W. Corb, R. C. O'Handley, S. Paradis, and N. J. Grant. *J. Appl. Phys.* 55:1781, 1984.

25. Reversible structural transformation in cobalt-base amorphous alloys. R. C. O'Handley, B. W. Corb, and N. J. Grant. *J. Appl. Phys.* 55: 1808, 1984.

Papers submitted:

1) A. Saito and R. M. Latanision. NACE Corrosion Conference, April 1983.

2) A. Saito and R. M. Latanision. Corrosion Resistance of Microcrystalline Aluminum Alloys. 5th Int'l. Conf. on Metallic Corrosion, Toronto, June, 1983.

3) A. Saito and R. M. Latanision. Corrosion Resistance of 2024 and Li-containing 2024 Based Microcrystalline Aluminum Alloys. *Corrosion.*

4) A. Saito and R. M. Latanision. Corrosion Resistance of 2618 Microcrystalline Alloys. *Corrosion Science.*

END

DATE
FILMED

6-84

DTIC